ESTIMATION OF FIBER MORPHOLOGY IN ELECTROSPINNING OF POLYURETHANE SOLUTIONS

Baturalp YALCINKAYA

Nonwoven and Nanofibrous Material Department, Textile Engineering Faculty, Technical University of Liberec, Liberec, Czech Republic, EU, baturalpyalcinkaya@hotmail.com

Abstract

Electrospinning of solution of Polyurethane in various concentrations and various tetraethylammonium bromide additives in dimethylformamide carried out under different voltages and jet current were measured. The effects of surface tension, viscosity, conductivity of solutions and applied voltages on the fiber morphology were investigated. The feed rate was kept constant during experiments. Result showed that surface tension and viscosity of solution had no effect on the jet current. However they had significant effect on jet forming and their morphologies. On the other side conductivity and applied voltage play important role on both the jet current and morphologies while by increasing the solutions conductivity and applied voltage the jet current was increased. During electrospinning of polyurethane solutions, six jet regimes were observed. The result of measured jet current show that all jet regimes had specific diagram of currents and believed that diagram of current lead the way to estimate fiber morphology.

Keywords: Electrospinning; solution jet regimes; jet current; nanofibers, fiber morphology

1. INTRODUCTION

Over the last two decades electrospinning process became one of the most preferred methods to intention for reaching submicron scale on fiber diameter. Studies in recent years are indicated that electrospun fiber forming method stands the test of time. It is possible to find great number of work about parameters which affects the electrospun fiber properties. These parameters are involved two groups, solution parameters such as surface tension [1], viscosity [2], conductivity [3] and process parameters such as applied voltage [4], distance between collector [5] and shape of the collector [6], tip of needle [7] and flow rate [8, 9].

There are many studies about range of electrospinning application such as filters [10], membranes [11], drug delivery and scaffold [12, 13]. Besides, many studies are focused mechanisms of the fluid properties at the tip of needle. Develop a theoretical framework for understanding the physical mechanisms of electrospinning documented by Hohman et al [14, 15] and Shin et al [16, 17]. Both studies were suggested whipping instability that bending and stretching of the jet. In the study of jet current, Kim et al. [18] and Bhattacharjee et al. [19] identified two distinct components of the total measured current, one linked with the transport of mass and its conductivity, the other with secondary electrospray emanating from the surface of the jet.

In this paper effect of applied voltage and solution properties on the jet current was investigated during electrospinning of various concentrations and salt additive of PU solutions, point-plate collector was used. Six jet regimes were observed as compared with previously study [20, 21, 22]. In here it is determined that every jet regimes had specific current diagram and every current diagram represented specific fibers structure. Hence it is believed that by using real time current measurement on the electrospinning of PU solutions can be used to estimate for structure of end product (fabric based on nanofibers).

2. EXPERIMENTAL

Polyurethane (PU) with molecular weight 2.000 g/mole was purchased from Larithane Company, dimethylformamide (DMF) and tetraethylamonium bromide (TEAB) was procured Fluka and Sigma Aldrich

Company. The polymer solution was prepared by dissolving PU in DMF. Polymer solutions of various weight percentage (15-17.5 and 20 wt. %) were prepared and for all PU solutions TEAB salt was added in various concentrations such as 0-0.4-0.8 and1.27 wt. %.

Ere electrospinning process, solution properties were determined. Conductivity and surface tension properties were measured by a conductivity meter (Radelkis, OK-102/1) and (Krüss) using a platinum plate and a highly precise electronic balance respectively. Rheological properties of polyurethane solutions were measured using Rheometer HAAKE RotoVisco 1. Polyurethane solutions were spun via needle electrospinning method. The environmental and process parameters were given Table 1.

Table 1 Spinning Parameters

Environmental Parameters		**Process Parameters**				
Temperature (^{0}C)	Humidity (%)	Distance between electrode (mm)	Feed Rate (ml/h)	Nozzle Protrusion (mm)	Voltage (kV)	Needle Outer Dia. (mm)
23	25	150	0,5	8	15-20-25	0,6

The electrospinning setup (**Fig. 1**) involved plastic plate and metal collector (point-plate) that was placed vertically parallel, syringe pump and high voltage supplier. Sensitive pump with needle was fixed perpendicular to the center of plastic plate. High voltage supplier was connected to needle. The current is evaluated by measuring the voltage on the resistor R (9811 Ω) placed between the collector electrode and ground. The voltage is measured by a 33401A digital multimeter produced by Agilent and stored on a computer at selected points on the time axis (approximately 20 records per second). Data's were re-evaluated using ohm law.

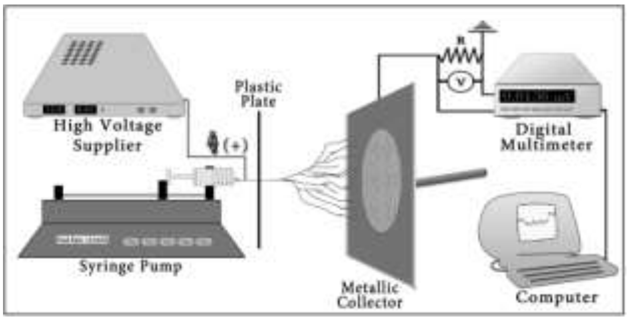

Fig 1 Electrospinning setup

Camera (Sony NEX-VG10E) record was taken at the same time with electrospinning process and current measurement for determining jet regimes using photographic video. The fiber morphology and diameter of the polyurethane nanofibers were determined using a scanning electron microscopy (SEM) TESCAN Digital Microscopy. Subsequently the average fiber diameter was calculated from the SEM images with NIS Element AR (Nikon) computer software.

3. RESULT AND DISCUSSION

Various concentration of PU in DMF and their salt additive solutions were electrospun at different applied voltages and jet current was measured. All experiments were performed under same environmental and given process (**Table 1**) conditions. In addition dry nanofibers as an end product were obtained from all electrospinning process.

Firstly, solution properties such as surface tension, conductivity and viscosity were determined and analyzed. **Fig. 2** is shown effect of PU and TEAB salt concentration on surface tension, viscosity and conductivity respectively. As shown in **Fig. 2** the surface tension was increased with increasing PU concentration however there is no significant change in surface tension values with TEAB salt concentration. On the other side as shown in **Fig. 2**, it is observed that important changes in viscosity and conductivity of solution's which were increased with increasing of PU and TEAB concentration were observed.

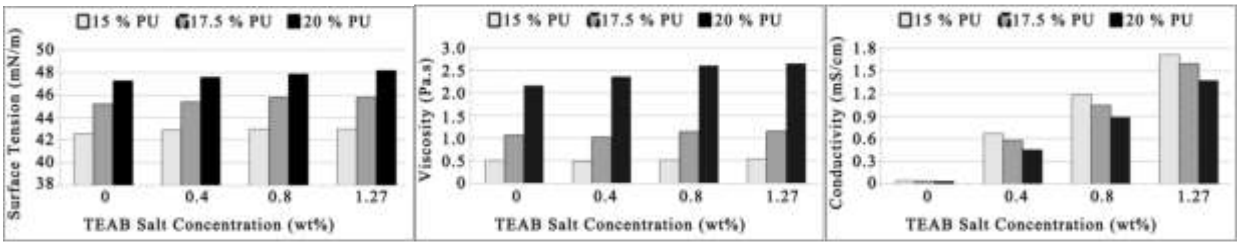

Fig. 2 Surface tension, viscosity, conductivity of PU solutions

Solutions which contain dissolved TEAB salts were able to increase conductivity of solution because of ions which were able to carry charge in their structure. On the other hand conductivity decreased with increment of PU concentration because the mobility of ions in the solution decreased with increasing of viscosity. In the literature same result were also obtained [24].

In the electrospinning process, by applying different voltages to various PU solutions, six jet regimes were reflected to photographic video, (a) 'stable jet', (b) 'irregular stable jet', (c) 'fluctuating jet', (d) 'stable jet with polymer drops', (e) 'stable jet starting after polymer drops', (f) 'stable jet starting after polymer drops then spinning finish after a while'. Multimeter measured different current values and each six different jet regimes presented unique current diagram behaviors. Each of them presented indicative properties and current result reflected to screen of the computer (**Fig. 3**).

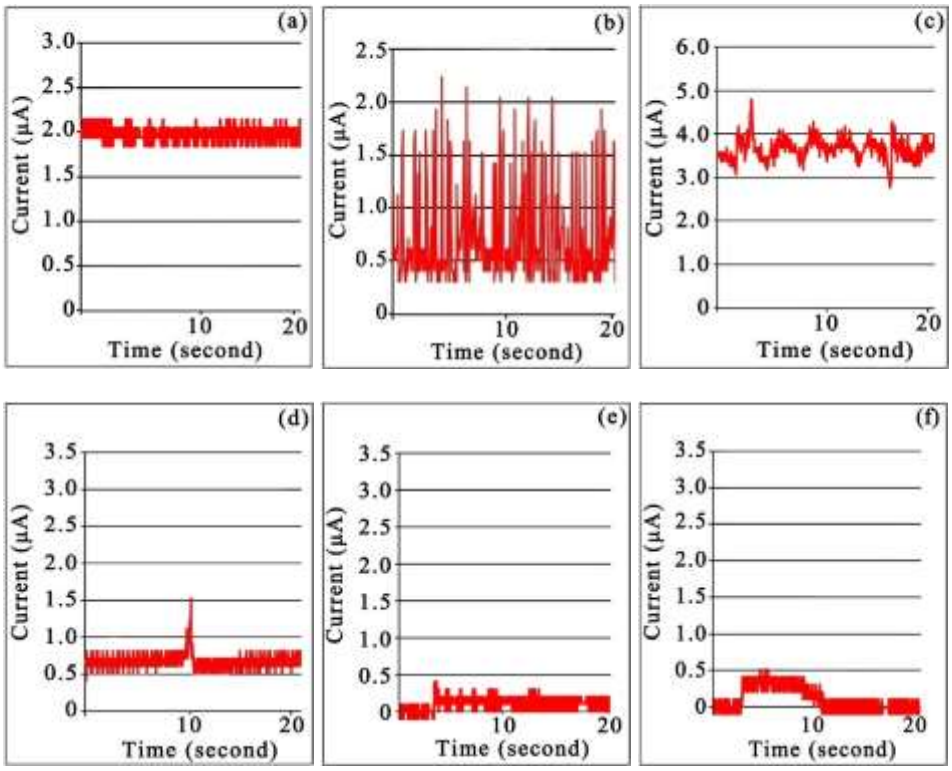

Fig. 3 Jet current versus time and types of jet regimes

It is obvious from **Fig. 3** that each jet regimes had different jet current behaviors. In generally stable jets (a) were observed at high applied voltage (20kV-25kV) and high concentration of PU (17.5 – 20 wt. %) (**Table 2**). In this jet regime, the polymer solutions reached tip of the needle, subsequently the solution is taken shape of Taylor cone or jet. Stable jet has regular electric current diagram so that means flow rate of solution is equal to the spinning process. Moreover SEM image of stable jets indicates that there is no non-fibrous area and beads (**Fig. 4**). Thin nanofibers were obtained at low viscosity of PU solutions and thick nanofibers were obtained high viscosity of PU solutions (**Table 3**). Hence fiber diameters of jet regime *a* is depended to concentration of solutions and additives.

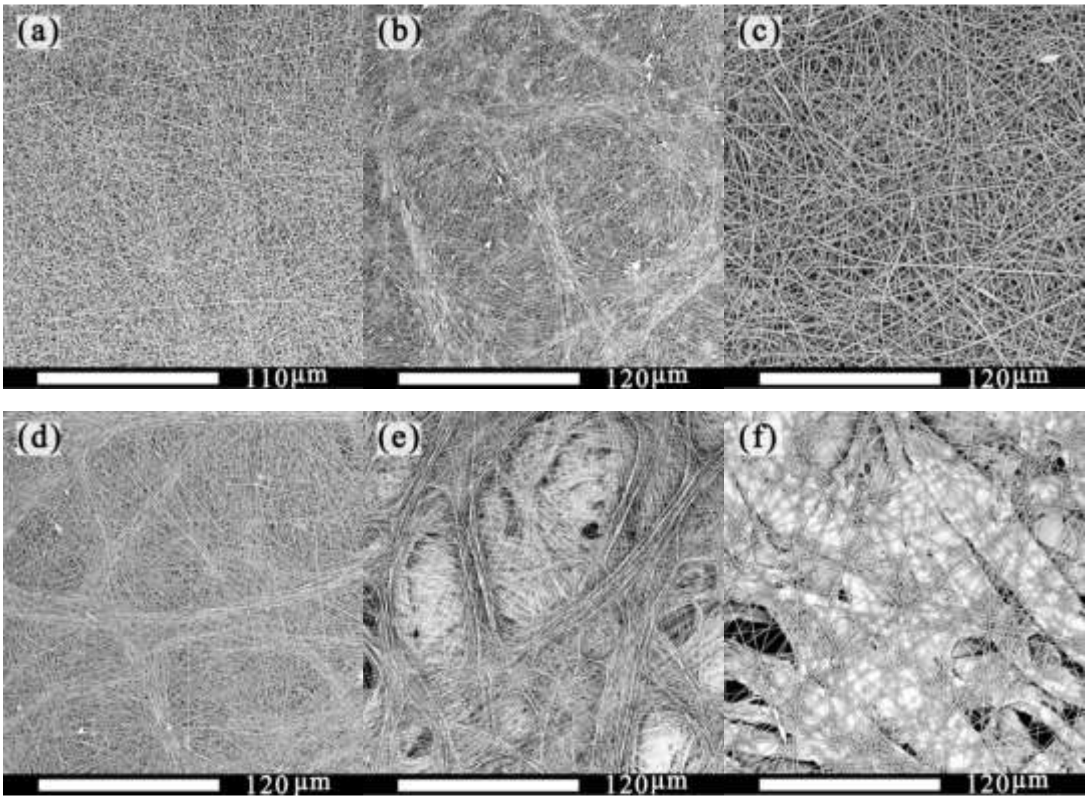

Fig. 4 SEM images of six different jet regimes

An irregular stable jet regime is denoted by letter *b* in **Fig. 3**. This regime was obtained only 25 kV applied voltage with 15 % wt PU concentration and its salt additive solutions (**Table 2**). This regime showed the characteristic of stable jet, however the direction of jet was changed frequently during the electrospinning for this reason electric current of this regime was reflected unorderly in **Fig. 3**. Low viscosity and surface tension of 15 wt. % PU solutions had highest solution conductivity hence high electric charge in the solution affected jet on tip needle negatively and jet regime *b* presented unstable equilibrium. Disorder on the jet regime *b* caused several beads (**Fig. 4**). However jet regime *b* was obtained by low PU concentration and at 25kV for this reason diameter of nanofiber were thin (**Table 3**).

Jet regime *c* represented the fluctuating jet. This regime was observed only 25kV and 20kV with highest viscosity and salt concentration (20 wt. % PU + 1.27 TEAB). Jet regime *c* showed irresolute structure at the tip of the needle in other word the spinning process created Taylor cone but there was no typical long jet on the tip of needle and the Taylor cone only bifurcated thick jet. Moreover narrow and wide bifurcated jet was observed during electrospinning process so that this fluctuation was reflected to **Fig. 3** as undulate. SEM image shows that the fiber diameter is thick and formless because high viscosity of PU and insufficient, shapeless jet structure (**Table 3**).

A stable jet with polymer drops regime is denoted by letter *d*. This regime type was observed at low applied voltage (15kV – 20kV) with all PU concentration (15 – 17.5 – 20 wt %) (**Table 2**). Low applied voltage was not able to reached speed of flow rate in the spinning process. Thus polymer solution was piled at the tip of the needle elliptically while electrospinning was processing. While polymer solution at the tip of the needle grew enough, it was succumbed to gravity and applied voltage hence it was fallen on the collector. It can be observed from the Figure 3 there is small peak in the current since the polymer droplet carries more charges than the jet [23].

Table 2 Electric current and regimes of jet

PU solutions	Avarage current *(μA) (15kV)*	Avarage current *(μA) (20kV)*	Avarage current *(μA)(25kV)*
15 wt. % PU	0,073 *(d)*	0,153 *(a)*	0,780 *(b)*
15 wt.% PU+0,4 wt.% TEAB	0,084 *(d)*	0,443 *(d)*	1,646 *(b)*
15 wt.% PU+0,8 wt.% TEAB	0,098 *(e)*	0,690 *(d)*	1,777 *(b)*
15 wt.% PU+1,27 wt.% TEAB	0,146 *(e)*	0,826 *(d)*	2,294 *(b)*
17,5 wt. % PU	0,095 *(d)*	0,298 *(a)*	1,137 *(a)*
17,5 wt.% PU+0,4 wt.% TEAB	0,110 *(e)*	0,526 *(a)*	2,002 *(a)*
17,5 wt.% PU+0,8 wt.% TEAB	0,164 *(d)*	0,700 *(d)*	2,072 *(a)*
17,5 wt.% PU+1,27 wt.% TEAB	0,212 *(e)*	0,837 *(d)*	2,555 *(a)*
17,5 wt. % PU	0,102 *(e)*	0,686 *(a)*	2,056 *(a)*
20 wt.% PU+0,4 wt.% TEAB	0,202 *(f)*	1,141 *(a)*	2,646 *(a)*
20 wt.% PU+0,4 wt.% TEAB	0,311 *(f)*	1,426 *(d)*	3,072 *(a)*
20 wt.% PU+0,4 wt.% TEAB	0,424 *(f)*	1,481 *(c)*	3,618 *(c)*

Fig. 4 shows the SEM image of the few fibers with beads obtained under jet regime of polymer droplet. Other side the structure of stable jet in this regime reflected as a fine fiber on the SEM image. There are not so much beads on the SEM image as well as irregular stable jet regime because beads were covered by fine fiber (**Table 3**). Moreover SEM images which is belong to jet regime *d* that some part had sticky fiber because of solution droplets.

In another jet regime which is unnamed in literature was denoted by letter *e*. This regime was obtained only at 15 kV applied voltage and stable jet was observed after polymer solution drops. (**Table 2**). Electrical force is not able to overcome surface tension of polymer solutions due to low voltage when voltage supplier switched on. Thereby polymer solution was piled at the tip of the needle at the beginning of process. When solution droplet grew enough on the needle tip, the solution droplet was fallen on collector and spinning process occurred. **Fig. 3** illustrated that beginning of the spinning electric current was zero subsequently there was a small surge in the current which was corresponding to falling of drop on the collector. SEM image of jet regime *e* shows fine fibers (**Table** 3) because of stable jet however there was some sticky fiber on the layers surface because of solution droplets. This jet regime had another disadvantage that low spinning productivity (**Fig. 4**).

Last jet regime is also inexistent in literature which was denoted by letter *f*. This regime was observed only at 15kV applied voltage with 20 wt. % PU concentration and its salt additive solutions (0.4 - 0.8 – 1.27) (**Table 2**). This regime has stable jet but it stars after polymer solution fall on collector subsequently due to the high viscosity and surface tension, then the electrospinning process stopped after a while. It is obvious in **Fig. 3** that electric current shows zero for a while then electric current is increasing when solution droplet reaches the collector. Finally electric current shows again zero value together with end of the spinning. SEM image of jet regime *f* is obviously shown that insufficient spinning productivity and thick fiber (**Fig. 4**, **Table 3**).

Table 3. Average fiber diameter of nanofibers

PU solutions	Average fiber diameter *(15kV)*	Average fiber diameter *(20kV)*	Average fiber diameter (*25kV)*
15 wt. % PU	153 ± 27 *(d)*	180 ± 27 *(a)*	193 ± 27 *(b)*
15 wt.% PU+0,4 wt.% TEAB	166 ± 29 *(d)*	185 ± 28 *(d)*	199 ± 33 *(b)*
15 wt.% PU+0,8 wt.% TEAB	156 ± 24 *(e)*	202 ± 32 *(d)*	209 ± 28 *(b)*
15 wt.% PU+1,27 wt.% TEAB	185 ± 26 *(e)*	208 ± 20 *(d)*	211 ± 22 *(b)*
17,5 wt. % PU	231 ± 38 *(d)*	246 ± 47 *(a)*	258 ± 47 *(a)*
17,5 wt.% PU+0,4 wt.% TEAB	245 ± 30 *(e)*	252 ± 27 *(a)*	273 ± 42 *(a)*
17,5 wt.% PU+0,8 wt.% TEAB	254 ± 34 *(d)*	265 ± 33 *(d)*	285 ± 32 *(a)*
17,5 wt.% PU+1,27 wt.% TEAB	256 ± 35 *(e)*	278 ± 37 *(d)*	295 ± 38 *(a)*
17,5 wt. % PU	439 ± 99 *(e)*	452 ± 53 *(a)*	463 ± 90 *(a)*
20 wt.% PU+0,4 wt.% TEAB	458 ± 62 *(f)*	470 ± 52 *(a)*	480 ± 56 *(a)*
20 wt.% PU+0,4 wt.% TEAB	475 ± 61 *(f)*	496 ± 90 *(d)*	506 ± 71 *(a)*
20 wt.% PU+0,4 wt.% TEAB	506 ± 72 *(f)*	522 ± 131 *(c)*	561 ± 95 *(c)*

As mentioned above, different applied voltage together with various solution properties exhibited specific impression on jet regimes and jet currents. It is believed that jet currents were represented jet regime and specified them as a fingerprint. Moreover fiber morphologies and fiber thickness are affected by jet regimes. Therefore current diagram on the computer screen provided to estimation of fibers structure during electrospinning process.

It is a fact accepted by author that measured current values are increased on the solution jet by increasing applied voltage on the needle electrospinning process. In literature same results are also obtained using different kind of polymer and solutions [14, 15] and Shin et al [16, 17]. The values on the Table 2 prove this general judgment. Otherwise Table 2 is shown that by increasing salt concentration in the same concentration of PU solutions increases current value on the solution jet. This result is also what is expected. However the Table 2 gives something which is never predicted. The values on the jet current were increasing when the PU concentration increased in constant salt concentration while conductivity decreased. In this case, it is believed that fiber diameter is related with jet diameter. If jet diameter increase therefore amount of the charge carrier are increased together with fiber diameter hence jet current is also increased. This phenomenon will investigated on the future work.

4. CONCLUSION

Various concentration of PU in DMF and their salt additive solutions were electrospun using needle electrospinning at different applied voltages and jet current was measured. Characteristics of jet were investigated via photographic video. As a consequence six type of jet were observed. At higher voltages stable, irregular stable and fluctuating jet regimes were observed. At low voltages and high surface tension and viscosity, stable jet regimes with droplets and its derivatives were observed. All jet regimes showed specific current diagram in addition the investigation of SEM images showed that all jet regimes exhibited specific characteristics. Hence by measuring jet current, fibers morphology of the nanofibers could also be estimated.

ACKNOWLEDGEMENTS

The authors are thankful to Ministry of Education, Youth and Sports of the Czech Republic (Student's grant competition TUL in specific University research in 2014 - Project No. 21041)" for their financial support.

REFERENCES

[1] Fong, H., Chun, I., & Reneker, D. H. (1999). Beaded nanofibers formed during electrospinning. *Polymer, 40*, 4585–4592.

[2] Jun Jun, Z., Hou, H. Q., Schaper, A., Wendorff, J. H., & Greiner A. (2003). Poly-Llactide nanofibers by electrospinning influence of solution viscosity and electrical conductivity on fiber diameter and fiber morphology. *e-Polymers, 009* 1-9.

[3] Kim, S. J., Lee, C. K., & Kim, S. I. (2005). Effect of ionic salts on the processing of poly(2-acrylamido-2-methyl-1-propane sulfonic acid) nanofibers. *Journal of Applied Polymer Science, 96,* 1388-1393.

[4] Fridrikh, S. V., Yu, J. H., Brenner, M. P., & Rutledge, G. C. (2003). Controlling the fiber diameter during electrospinning. *Physical Review Letters, 90,* :144502.

[5] Baker, S. C., Atkin, N., Gunning, P. A., Granville, N., Wilson, K., Wilson, D., & Southgate, J. (2006). Characterisation of electrospun polystyrene scaffolds for three-dimensional in vitro biological studies. *Biomaterials, 27,* :3136–3146.

[6] Zussman, E., Rittel, D., & Yarin, A. L. (2003). Failure modes of electrospun nanofibers. *Applied Physics Letters, 82,*3958-3960.

[7] Berkland, C., Pack, D.W., & Kim, K. K. (2004). Controlling surface nano-structure using flow-limited field-injection electrostatic spraying (FFESS) of poly(D,Llactide- co-glycolide). *Biomaterials, 25,* :5649–5658.

[8] Jeun, J. P., Lim, Y. M., & Nho, Y. C. (2005). Study on morphology of electrospun poly(caprolactone) nanofiber. *Journal of Industrial and Engineering Chemistry 11,* :573–578.

[9] Buttafoco, L., Kolkman, N. G., Engbers-BuZjtenhuijs, P., Poot, A. A., Dijkstra, P. J. Vermes, I., & Feijen, J. (2006). Electrospinning of collagen and elastin for tissue engineering applications. *Biomaterials, 27,* 724– 734.

[10] Shin, C., Chase, G. G., & Reneker, D. H. (2005). Recycled expanded polystyrene nanofibers applied in filter media. *Colloids and Surfaces A: Physicochemical and Engineering Aspects, 262*, 211–215.

[11] Ding, B., Yamazaki, M., & Shiratori, S. (2005). Electrospun fibrous polyacrylic acid membrane based gas sensors. *Sensors and Actuators B: Chemical, 106*, 477–483.

[12] Murugan, R., & Ramakrishna, S. (2006). Nano-featured scaffolds for tissue engineering: a review of spinning methodologies. *Tissue Engineering, 12*, 435–447.

[13] Zhang, Y. Z., Lim, C. T., Ramakrishna, S., & Huang, Z.M. (2005). Recent development of polymer nanofibers for biomedical and biotechnological applications. *Journal of Materials Science: Materials in Medicine, 16*, 933–946.

[14] Hohman, M. M., Shin, M., Rutledge, G., & Brenner, P. M. (2001a). Electrospinning and electrically forced jets. I. Stability theory. *Physics of fluids, 13,* 2201-2220.

[15] Hohman, M. M., Shin, M., Rutledge, G., & Brenner, P.M. (2001b). Electrospinning and electrically forced jets. II. Stability theory. *Physics of fluids, 13,* 2221- 2236.

[16] Shin, Y. M., Hohman, M. M., Brenner, M. P., & Rutledge, G. C. (2001a). Electrospinning: a whipping fluid jet generates submicron polymer fibers. *Applied Physics Letters 78,* 1149 1151.

[17] Shin, Y. M., Hohman, M. M., Brenner, M. P., & Rutledge, G. C. (2001b). Experimental characterization of electrospinning: the electrically forced jet and instabilities. *Polymer 42*, 9955–9967.

[18] Kim, S. J., Lee, C. K., & Kim, S. I. (2004). Effect of ionic salts on the processing of poly(2-acrylamido-2-methyl-1-propane sulfonic acid) nanofibers, *Journal of Applied Polymer Science, 96*, 1388–1393

[19] Bhattacharjee, P. K., Schneider, T. M., Brenner, M. P., McKinley, G. H., & Rutledge, G. C. (2010). On the measured current in electrospinning, *Journal of Applied Physics, 107*, 044306.

[20] Fallahi, D., Rafizadeh, M., Mohammadi, N., & Vahidi, B. (2009). Effects of feed rate and solution conductivity on jet current and fiber diameter in electrospinning of polyacrylonitrile solutions. *E-Polymers, 104,* 1618-7229.

[21] Samatham, R., & Kim, K,J. (2006). Electric Current as a Control Variable in the Electrospinning Process. *Polymer Engineering and Science,10,* 954- 959.

[22] Fallahi, D., Rafizadeh, M., Mohammadi, N., & Vahidi, B. (2008) Effect of applied voltage on jet electric current and flow rate in electrospinning of polyacrylonitrile solutions, *Society of Chemical Industry, Polym Int* 0959– 8103.

[23] Yalçınkaya, B., Yener, F., Cengiz-Çallıoğlu, F., & Jirsak, O. (2012, October). *Effect of concentration and salt additive on Taylor cone structure*, Paper presented at 3rd NanoCon, Brno Czech Republic.